INSTITUTE OF PHYSICS PUBLISHING PHYSICS IN MEDICINE AND BIOLOGY

Phys. Med. Biol. **47** (2002) N17–N24 PII: S0031-9155(02)26093-5

NOTE

Rapid generation of preview images for real-time 3D MR angiography

Oliver Wieben[1,2], **Timothy J Carroll**[2], **J Shannon Swan**[3,4] **and Richard Frayne**[2,3,5,6]

[1] Department of Electrical and Computer Engineering, University of Wisconsin-Madison, WI, USA
[2] Department of Medical Physics, University of Wisconsin-Madison, WI, USA
[3] Department of Radiology, University of Wisconsin-Madison, WI, USA

E-mail: rfrayne@ucalgary.ca

Received 25 June 2001
Published 12 December 2001
Online at stacks.iop.org/PMB/47/N17

Abstract

In 3D real-time MR angiography the reconstruction of images from large raw datasets via Fourier transforms with minimal delays is problematic. In this study strategies for reconstructing time-resolved three-dimensional (3D) datasets at a rate substantially faster than conventional 3D MR image reconstruction were investigated on general-purpose computer hardware. Moderate quality 'preview images' were generated from *k*-space subsets to reduce image reconstruction times from more than 50 s to 0.3 s per image volume. A blinded review of 3D TRICKS patient examinations showed that these moderate-quality images were sufficient for providing immediate feedback and guiding the subsequent reconstruction of selected time frames ($p < 0.05$). Fourier projection (reconstruction from a central *k*-space slice) was the most efficient reconstruction technique. However, the reduction of the reconstructed volume in all three dimensions resulted in higher contrast and better image quality while allowing reconstruction in near-to-real-time (less than 1 s per image volume). The use of such preview images in a real-time system allows for fast feedback from dynamic 3D datasets, enables scanner interaction with minimal latencies and can substantially reduce the postprocessing times.

[4] Now at the Department of Radiology, Indiana University, Indianapolis, IN, USA.
[5] Now at the Departments of Radiology and Clsdatyinical Neurosciences, University of Calgary, Calgary, AB, Canada.
[6] Present Address: Seaman Family MR Centre, Foothills Medical Centre/University of Calgary, 1403 29th Street NW, Calgary AB Canada T2N 2T9.

0031-9155/02/010017+08$30.00

1. Introduction

The use of T_1 shortening contrast agents in combination with high-performance gradient systems allows for the acquisition of three-dimensional MR angiography (MRA) datasets with ultra-short repitition times (TR). Our group is developing an interactive, real-time system for time-resolved MRA (Block *et al* 1999) based on 3D TRICKS (Korosec *et al* 1996, Frayne *et al* 1997) acquisitions to mimick some of the features of x-ray DSA. A major obstacle is that a standard 3D image reconstruction on current general-purpose hardware platforms cannot keep up with the rate of data acquisition, particularly when large data volumes are acquired using multiple receiver coils. We have reduced the latency between scan completion and display of a peak arterial time frame to minutes using contrast uptake information extracted directly from the *k*-space (Carroll *et al* 2000). However, this must be performed retrospectively and does not provide near-real-time feedback as it is essential in dynamic 3D imaging, for example, to synchronize specific data acquisition or initiate a breath-hold with the contrast arrival in an area of interest.

Simplistically, the delay between data acquisition and display of MR images is primarily due to the time required for data transfer and image reconstruction, of which the latter is mainly spent on the calculations of Fourier transforms (FTs) in the case of acquisitions on a Cartesian grid (Zhou *et al* 1999). With adequate data transfer bandwidth, speed of the image reconstruction becomes the crucial step. Riederer *et al* (1988, 1993) implemented a real-time MRA system for clinical use where a 2D slice is regularly acquired and reconstructed on custom hardware before and during the acquisition of one 3D volume. The use of distributed systems (Kerr *et al* 1997) or multiple dedicated processors (Weber *et al* 1999) has been recently proposed for fast reconstructions in 2D imaging with minimal delays.

3D TRICKS uses view sharing, data interpolation and zero-filling to generate multiple large three-dimensional datasets, which significantly increases reconstruction complexity over other time-resolved acquisitions. We investigated methods to generate 2D projection images from the 3D volumes on a single workstation at rates substantially faster than those required for a full reconstruction. These *preview images* tend to be of lower image quality because they are reconstructed from *k*-space subsets. However, we hypothesize that they provide sufficient information to detect contrast arrival and show complex vessel filling. They can be used to synchronize data acquisition with arterial enhancement and to reduce postprocessing times by identifying critical time frames such as the peak arterial frame or a frame for mask mode subtraction to guide the subsequential high-quality reconstruction. Also, in the abdominal region the typical breath-hold can be initiated in response to the detected bolus arrival instead of methods with potentially more uncertainties such as the use of a test bolus. This approach is an alternative to solutions which require expensive dedicated hardware. The preview images discussed below differ in the fraction of reconstructed *k*-space data, the number of operations needed for reconstruction and their reconstructed spatial resolution. They are compared in terms of (1) reconstruction time, (2) image contrast in maximum-intensity-projection (MIP) images and (3) a subjective evaluation of image quality.

2. Theory

The number of operations required for FT calculations and hence reconstruction time can be decreased if the reconstructed image volume is reduced from $V = N_x \times N_y \times N_z$ to $V' = N'_x \times N'_y \times N'_z$, where $N'_x \leqslant N_x$ and $N'_y \leqslant N_y$ and $N'_z \leqslant N_z$. Figure 1 shows two 1D examples of *k*-space subsets used for the generation of preview images. In method A, only the central contiguous part of the *k*-space data is used. This corresponds to a low-pass filtered

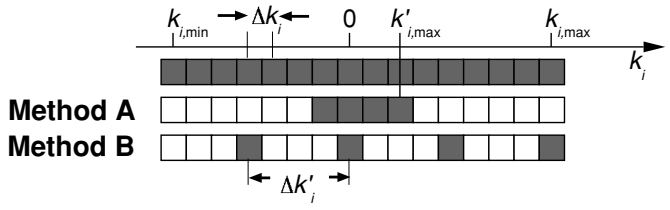

Figure 1. Sampling schemes for low-pass filtered (method A), and reduced FOV k-space subsets (method B) with $N'_i = 4$, where i denotes an arbitrary direction (x, y, z). The grey elements represent actual sampling points for each method.

dataset with decreased spatial resolution, $\Delta i = 1/k'_{i,\max}$, in the i-direction. The truncation can be applied in all three dimensions in k-space simultaneously but reduces resolution and may introduce ringing artifacts in the images.

In method B, a higher spatial resolution is achieved; however, this comes at the expense of a reduced FOV ($FOV_i = 1/\Delta k'_i$), when every mth data point ($m = N_i/N'_i$) is sampled in i. In order to achieve reduction in all three dimensions, method B can be applied in one dimension (typically the MIP direction in 3D TRICKS) while low-pass filtered data (method A) are used in the other two dimensions. It is beneficial to reduce the data in k_x and k_y by the same factor (i.e. $N_x/N'_x = N_y/N'_y$) in order to maintain square pixels in the reconstructed slices.

A special case of the reduction of k-space is the reconstruction from a single slice ($N'_z = 1$). It can be derived from the central-slice theorem that the inverse FT of a plane passing through the origin in k-space is equivalent to an integration of the data perpendicular to the plane in image space (Mersereau and Oppenheimer 1974). This reconstruction can be implemented very efficiently as it is reduced from a 3D to a 2D task (Napel *et al* 1991).

3. Methods

3.1. Data acquisition and image reconstruction

3D TRICKS rapidly acquires a series of data volumes before, during and after the passage of a venously injected contrast agent through the arteries of interest (Korosec *et al* 1996, Frayne *et al* 1996). The pulse sequence is based on a rf-spoiled gradient-recalled echo sequence and combines various fast-scanning elements including variable rate k-space sampling (Doyle *et al* 1995), view sharing and temporal interpolation (Riederer *et al* 1988, van Vaals *et al* 1993) and zero filling (Du *et al* 1994). 3D TRICKS allows for the acquisition and reconstruction of high-quality volume MRA images at a frame rate of 2 to 9 s, the exact rate is dependent on the selected imaging parameters.

Ten consecutive 3D TRICKS thigh examinations of patients (all male, average age = 59.2 years) were selected for this study. The data acquisition parameters were: flip angle = 45°, TR = 7.6 ms, TE = 1.6 ms, acquisition matrix $V_a = 312 \times 144 \times 24$, reconstruction matrix $V = 512 \times 384 \times 48$, reconstructed frame rates $\Delta t = 6.5$ to 9.0 s, number of time frames = 15–20, FOV = 480 mm × 360 mm, slab thickness = 72–168 mm, four-channel phased-array coils, 7–20 ml Gadodiamide (Omniscan, Nycomed, Princeton, NJ) at 0.5–1.5 ml s^{-1}. Imaging was performed on a clinical 1.5 T scanner (Signa 5.X, General Electric Medical Systems, Waukesha, WI) and the contrast was administered using a power injector (Spectris, Medrad, Pittsburgh, PA). This was the second injection in a three-station

exam and a previous injection of 0.1 mmol kg^{-1} was used to image the abdomen. Written, informed consent was obtained from all patients prior to the examination.

The acquired data volume V_a (up to 400 Mb for one exam) was transferred from the scanner to a workstation (Ultrasparc II, Sun Microsystems, Palo Alto, CA). 15 to 20 complex image volumes V were reconstructed with 3D Fourier transforms and displayed after calculating MIP images from the source magnitude images. The computational efforts were minimized by choosing the optimal order of the 1D FTs, which varies with the relative increase in each dimension from the acquired to the reconstructed volumes. The 1D FTs were efficiently calculated for any array lengths by the FFTW software package (Frigo and Johnson 1998). Mask-mode subtraction was used for improved delineaton of vessels from the background. Complex subtraction (CS) in k-space (Wang *et al* 1996) was performed rather than magnitude subtraction in image space because of the more efficient calculation.

3.2. Reconstruction time and image contrast

Time series of all patients were reconstructed with a full reconstruction and with methods A and B using different matrix sizes. CS was implemented using the first volume in the time series as the mask. The in-plane reconstructed matrix size was varied (512×384, 256×192, and 128×96). Further reductions resulted in images with an unacceptable in-plane resolution. The number of reconstructed slices was decreased from $N_z' = 48$ (full volume) to 32, 16, 8, 4, 2, and 1. Only $N_z' = 2$, 4, 8, and 16 slices were reconstructed with method B, since the reconstruction matrices for $N_z' = 1$, 32, and 48 are identical to method A. Combining methods A and B results in a total of 33 investigated k-space datasets. The mean reconstruction time per volume, $\langle T \rangle$, which is equivalent to the reconstructed frame rate, was obtained by averaging all reconstructed time frames over the ten patients for each matrix size.

Regions-of-interest (ROIs) were interactively defined on the MIP images obtained from the fully reconstructed image sets and analysed for all 33 datasets. The ROIs were placed on arteries and tissues located in the upper, middle and lower part of the thighs and used to determine image contrast from the MIP images of different reconstruction matrices. Measured image contrast varied due to patient-dependent hemodynamics and injection and imaging protocols. Therefore, the measured contrast curves were subsequently normalized by dividing by the corresponding contrast value from the images using the full reconstruction. A mean normalized contrast for each patient was found by averaging over all time frames after the arrival of the contrast. These results were finally averaged over the ten patients to $\langle C_{\mathrm{norm}} \rangle$.

3.3. Subjective evaluation

Four blinded reviewers evaluated images from the full reconstruction matrix (matrix M_{I}), a single k_z-slice (M_{II}) and three matrices with large time savings ($M_{\mathrm{III}} = 256 \times 192 \times 4$, method A; $M_{\mathrm{IV}} = 256 \times 192 \times 4$, method B; $M_{\mathrm{V}} = 128 \times 96 \times 4$, method B). Each observer reviewed 50 time series (10 patients $\times$ 5 reconstruction techniques) of MIP images with CS on film. For each time series, the observers were asked: (1) can you verify that the exam was technically successful (0 = No and 1 = Yes)? (2) could you use this time series of images to guide a complete reconstruction (0 = No and 1 = Yes)? (3) what is the peak arterial time frame? and (4) what is the overall image quality on a 5-point scale (1 = poor, 3 = adequate and 5 = excellent)?

The data from questions 1 and 2 (technical success and ability to guide a full reconstruction) were analysed using a Cochran Q-test to determine whether there were statistically significant differences among dichotomous nominal-scale results (Zar 1996). A

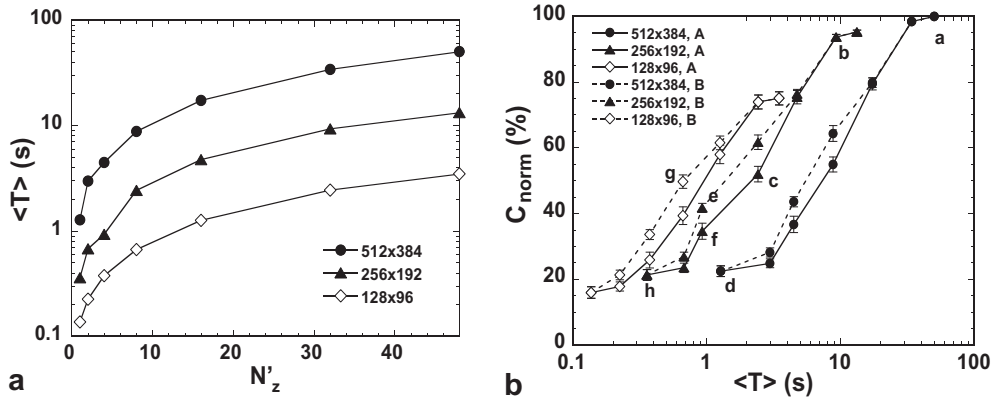

Figure 2. The mean reconstruction time per volume $\langle T \rangle$ can be significantly reduced when the number of sample points in the projection direction N'_z and the size of the in-plane matrix $N'_x \times N'_y$ is decreased (a). However, the mean normalized contrast $\langle C_{\text{norm}} \rangle$ also decreases with reduced reconstruction time (b). The labels in (b) refer to the example shown in figure 3.

multiple comparison procedure was used to determine which pair or pairs of techniques were different. The data from question 3 (peak arterial frame) was compared against the true peak arterial frame. True peak arterial frame was determined from a ROI analysis on the time series of images generated using the full reconstruction. A paired T-test was used to determine statistical differences between operator-determined and true peak arterial frame. The significance of differences in question 4 (overall image quality) was assessed using repeated measures one-way ANOVA to determine if differences in the reconstruction technique or in the operator had significant effects. A level of $p = 0.05$ was used as the threshold of statistical significance for all statistical tests.

4. Results

The mean reconstruction time per volume $\langle T \rangle$ is displayed for various matrix sizes in figure 2(a). While the full reconstruction takes more than 50 s per time frame, preview images from small matrices can be generated in less than 0.2 s. Fourier projections with low in-plane resolution require very few computations but the contrast drops to less than 20% of the mean normalized contrast $\langle C_{\text{norm}} \rangle$ obtained with full reconstruction (figure 2(b)). The contrast decreases when the in-plane resolution or the number of reconstructed slices is decreased.

Figure 3 shows images of a peak arterial frame reconstructed from different k-space subsets. The images are ordered by the reconstruction times per image volume, which were measured as 50.29, 9.31, 2.43, 1.28, 0.93, 0.93, 0.67, and 0.36 s, respectively.

The mean score of the subjective evaluation of the technical success ranged from 0.85 to 1.00 with matrices M_{I} and M_{IV} having a 100% acceptance ($M_{\text{II}} = 0.85 \pm 0.06$, $M_{\text{III}} = 0.95 \pm 0.03$, $M_{\text{V}} = 0.95 \pm 0.03$). Analysed over all reconstruction techniques, a statistically significant difference was found. Additional testing showed that the performance of the single slice preview technique (Fourier projection) was significantly worse than reconstructions from matrices I and IV. All other differences between pairs of reconstruction techniques were found to be not statistically significant. The ability to subsequently guide a full image reconstruction from the preview images was found to vary with the different preview image strategies. The mean scores for reconstruction guidance were 1.0 ± 0.0 (M_{I}), 0.90 ± 0.05 (M_{II}), 0.93 ± 0.04

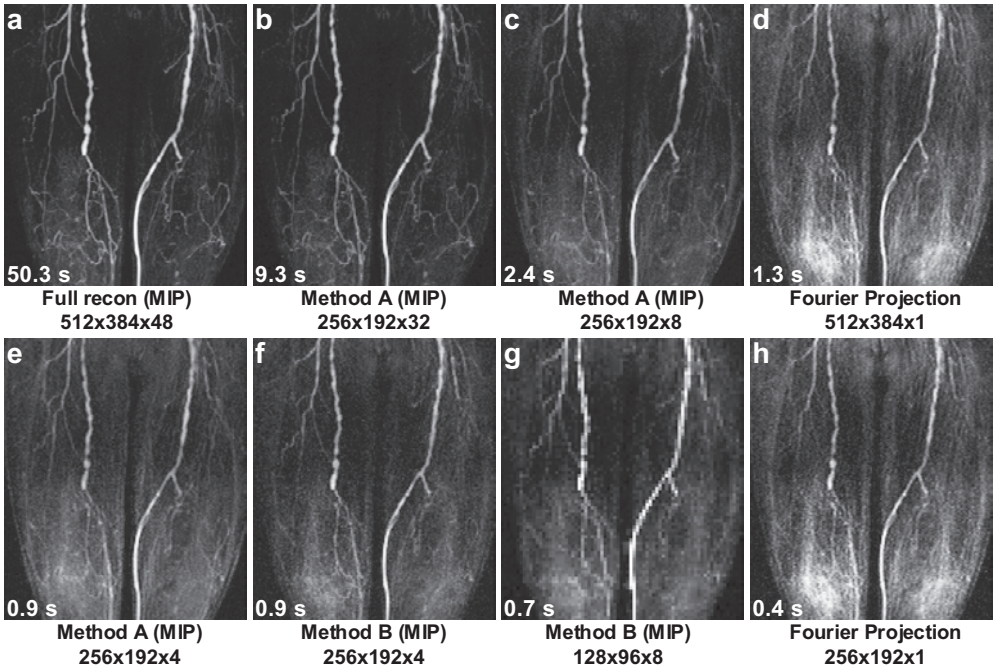

Figure 3. Projection images of a thigh examination (peak arterial time frame) reconstructed from different *k*-space datasets: full *k*-space volume 512 × 384 × 48 (a); 256 × 192 × 32 (b); Fourier projections 512 × 384 × 1 (d) and 256 × 192 × 1 (h); Method A with matrices of 256 × 192 × 8 (c) and 256 × 192 × 4 (e); and method B with matrices of 256 × 192 × 4 (f) and 128 × 96 × 8 (g). The images are ordered by the reconstruction times (MIP = maximum intensity projection).

(M_{III}), 0.98 ± 0.03 (M_{IV}), and 1.0 ± 0.0 (M_{V}). The Cochran Q-test indicated that differences did exist between the data; however, a subsequent multiple comparison test failed to show statistically significant differences between the scores for any pair of images.

The average difference between the mean peak arterial time frames for the analysed reconstruction methods was less than half a time frame and not statistically significant. The mean scores for overall image quality were statistically different and varied as follows: 4.7 ± 0.1 (M_{I}), 2.5 ± 0.2 (M_{II}), 3.2 ± 0.2 (M_{III}), 3.1 ± 0.2 (M_{IV}), and 2.3 ± 0.2 (M_{V}). The mean image quality scores for the four operators were (2.6 ± 0.2, 2.9 ± 0.2, 3.5 ± 0.2, 3.7 ± 0.1). The effect of changing operator and the interaction between operator and reconstruction technique were found to be significant. The inter-operator variability was smaller for the images generated by the full reconstruction (coefficient of variation, $\rho = 0.13$) than the four other techniques ($0.32 \leqslant \rho \leqslant 0.46$).

5. Discussion and conclusions

With method A, the displayed FOV is identical to the FOV of a complete reconstruction and the voxel dimension increases by a factor of $(N_x/N'_x) \times (N_y/N'_y) \times (N_z/N'_z)$ compared to fully reconstructed volumes. By decreasing N'_x, N'_y, or N'_z, the computational requirements for the generation of preview images decrease, but so does the delineation of details in the image. In particular, signals from small structures are obscured by regions of higher background signal

(e.g. at the knee) and partial volume effects become more evident in the images (compare figures 3(a) and (d), and (b), (c), (e) and (h)).

The voxel dimensions do not change for method B, but the FOV is reduced and aliasing in z is allowed to occur. Since the displayed images are MIP images, the aliasing in z is inconsequential. Method B (f) produces images with more vessel detail and better background suppresion than method A (e) when reconstructed from identical matrix dimensions (compare figures 3(e) and (f)). For identical reconstruction matrix sizes, method B also has an equal or larger contrast compared to method A. The preferred reconstruction scheme is a $128 \times 96 \times 8$ matrix with method B which provides the highest contrast for sub-second frame rates on our system.

Little variation in the normalized contrast measurements versus time frame (not shown) for the same reconstruction matrix indicates that the dynamics of the contrast enhancement is adequately depicted in the preview images. This was to be expected since the central region of k-space is kept and, therefore, most of the signal energy is preserved in the reconstructed subset. The subjective evaluation also demonstrated that all observers were able to correctly determine the peak arterial image from each time-series of images.

As expected, the blinded review showed the highest image quality for fully reconstructed images. Preview images are of lower quality but they are rapidly generated to reduce postprocessing times and to keep up with the data acquisition rate in real-time imaging. They are not intended to replace fully reconstructed diagnostic images. The inter-operator variabilities suggest that the operators mostly agreed with the image quality for the fully reconstructed images, but had different assessments when viewing the preview images. We anticipate, however, that with proper operator training the variation in image quality assessments would be reduced. We also hypothesize that the contrast and the scores for image quality would be higher if we would have chosen exams from another anatomic region with less background signal from fat and a previous injection, or a subject population with normal (faster) flow. Potentially, images reconstructed from a few thick slices or the Fourier projection will be degraded due to intra-voxel dephasing if the magnetic field homogeniety is poor.

Preview images are a crucial component for our dynamic 3D acquisition in the abdomen with a real-time system (Wieben *et al* 2001). MIP images from a $128 \times 96 \times 8$ matrix are updated with overall latencies smaller than 2 s on the workstation described above. The patient is asked to hold his breath upon contrast arrival in the left ventricle and shortly after a modified 3D TRICKS data acquisition is started in the abdomen.

In conclusion, this study shows that preview images based on the reconstruction of reduced matrices can generate useful images from 3D TRICKS datasets at high reconstruction rates. The blinded study has confirmed that preview images reconstructed at less than 1 s per image volume have sufficient quality to identify critical time frames and evaluate the technical success of a scan. Therefore, these images can be used to monitor contrast arrival, initiate a breath-hold and trigger different acquisition schemes for immediate feedback and interactive scan control. Reconstructions from k-space subsets reduced in three dimensions ($N_z' > 1$) have higher measured contrast and image quality grades than Fourier projections ($N_z' = 1$) due to decreased partial volume effects in the slice encoding direction. The reconstruction method that includes higher spatial frequencies in the slice encoding direction at the expense of potential spatial aliasing (method B) produced improved image contrast as compared to a method that only includes the lower spatial frequencies (method A). Our method of producing preview images is scalable so that the frame rate can be tailored to the acquisition parameters and the available computer ressources. Furthermore, this approach does not require any special-purpose hardware and can be easily implemented.

Acknowledgments

The authors gratefully acknowledge Charles A Mistretta, PhD, Walter F Block, PhD, and Frank R Korosec, PhD, for valuable discussions and contributions, and thank Bret J Borowski, RTR, for technical assistance.

References

Block W F, Carroll T J, Palmbach A W, Mistretta C A and Grist T M 1999 A real-time 3D MR digital subtraction angiography system *85th Scientific Assembly of the Radiological Society of North America (Chicago)* p 276

Carroll T J, Korosec F R, Swan J S, Grist T M, Frayne R and Mistretta C A 2000 Method for rapidly determining and reconstructing the peak arterial frame from a time-resolved CE-MRA exam *Magn. Reson. Med.* **44** 817–20

Doyle M, Walsh E G, Blackwell G G and Pohost G M 1995 Block regional interpolation scheme for k-space (BRISK): a rapid cardiac imaging technique *Magn. Reson. Med.* **33** 163–70

Du Y P, Parker D L, Davis W L and Cao G 1997 Reduction of partial-volume artifacts with zero-filled interpolation in three-dimensional MR angiography *Magn. Reson. Med.* **4** 733–41

Frayne R, Grist T M, Korosec F R, Willig D S, Swan J S, Turski P A and Mistretta C A 1996 MR angiography with three-dimensional MR digital subtraction angiography *Top. Magn. Reson. Imaging* **8** 366–88

Frigo M and Johnson S G 1998 FFTW: an adaptive software architecture for the FFT *'IEEE ICASSP' (Seattle)* vol 3 p 1381

Kerr A B, Pauly J M, Hu B S, Li K C, Hardy C J, Meyer C H and Macovski A 1997 Real-time interactive MRI on a conventional scanner *Magn. Reson. Med.* **38** 355–67

Korosec F R, Frayne R, Grist T M and Mistretta C A 1996 Time-resolved contrast-enhanced 3D MR angiography *Magn. Reson. Med.* **36** 345–51

Mersereau R M and Oppenheimer A V 1974 Digital reconstruction of multidimensional signals from their projections *Proc. IEEE* **62** 1319–38

Napel S, Dunne S and Rutt B K 1991 Fast Fourier projection for MR angiography *Magn. Reson. Med.* **19** 393–405

Riederer S J, Tasciyan T, Farzaneh F, Lee J N, Wright R C and Herfkens R J 1988 MR fluoroscopy: technical feasibility *Magn. Reson. Med.* **8** 1–15

Riederer S J *et al* 2000 Three-dimensional contrast-enhanced MR angiography with real-time fluoroscopic triggering: design specifications and technical reliability in 330 patient studies *Radiology* **215** 584–93

van Vaals J J *et al* 1993 'Keyhole' method for accelerating imaging of contrast agent uptake *J. Magn. Reson. Imaging* **3** (4)

Wang Y, Johnston D L, Breen J F, Huston J III, Jack C R, Julsrud P R, Kiely M J, King B F, Riederer S J and Ehman R L 1996 Dynamic MR digital subtraction angiography using contrast enhancement, fast data acquisition, and complex subtraction *Magn. Reson. Med.* **36** 551–6

Weber O M, Eggers H, Spiegel M A, Scheidegger M B, Proksa R and Boesiger P 1999 Real-time interactive Magnetic Resonance imaging with multiple coils for the assessment of left ventricular function *J. Magn. Reson. Imaging* **10** 826–32

Wieben O, Block W F, Grist T M and Mistretta C A 2001 Time-resolved 3D MR Angiography with a real-time system *Proc. ISMRM, 9th Annual Meeting and ESMRMB, 18th Annual Meeting (Glasgow)* p 737

Zar J H 1996 *Biostatistical Analysis* 3 edn (Saddle River, NJ: Prentice Hall)

Zhou Y, Skuldt D H and Frayne R 1999 Rapid reconstruction of 3D TRICKS images *Proc. ISMRM, 7th Annual Meeting (Philadelphia)* p 1655